J Inno Sci Eng, 2024, 8(2): 115-131
*https://doi.org/ 10.38088/jise.1270276*

Research Article

# Investigation of the Efficiency of Photovoltaic Thermal (PV/T) Hybrid Collector as Solution for Water Desalination Needs of Rural Areas in Niger

**Mariama Ali Garba** [1,*], **Bulent Yesilata** [1]

[1] *Department of Energy Systems Engineering, Faculty of Engineering and Natural Sciences, Ankara Yildirim Beyazit University, Ankara, Turkey*

Cite this paper as:
Garba, M.A. and Yesilata, B. (2024). *Investigation of the Efficiency of Photovoltaic Thermal (PV/T) Hybrid Collector as Solution for Water Desalination Needs of Rural Areas in Niger.*Journal of Innovative Science and Engineering. 8(2): 115-131

*Corresponding author: Mariama Ali Garba
E-mail: aligarbamariama@gmail.com

Received Date: 24/03/2023
Accepted Date: 17/09/2024


## Abstract

The efficiency of SS (single slope) solar still integrated with a Photovoltaic-thermal collector (PVT) is investigated underneath Niamey's climatic weather conditions. Thus, a theoretical study is conducted, and MATLAB software is used to simulate the equations and data of climatic conditions in Niamey. Three different months have been used for the computations. The electrical efficiency and thermal power of the PVT structure, along with the temperatures of water and glass cover are determined. Also, the daily freshwater yield and overall thermal efficiency of the system are calculated. As a result, the maximum electrical and thermal efficiencies of this structure at noon are found to be 14% and 58.09% respectively. The maximum temperature of water is recorded to be 60 °C while that of the glass cover is reported to be 51.4 °C. The highest freshwater production rate is observed to be 1.10 kg/m$^2$ per hour at noon time, and the daily freshwater yield is 2.62 kg/m$^2$.

*Keywords:* PVT, Single slope solar still, Desalination, Solar energy in Niger, PV hybrid, renewable energy

## 1. Introduction

The growing need for portable water is a notable concern, especially in isolated regions where the availability of potable water is restricted. Although 70% of the Earth's surface is submerged in water, most of this water is in the seas, rendering it unfit for consumption. In response to this problem, a desalination technique utilizing solar still has been developed to manufacture potable water [1]**.** This procedure entails the separation of minerals and salt from saline water, yielding potable water appropriate for both people and animals. Photovoltaic-thermal modules are the initial development technologies for hybrid solar systems that transform solar radiation into both thermal and electrical energy [2].

Niger, a nation located in West Africa and bordered by the Sahara Desert, has considerable potential in the field of solar energy, since it experiences an average sun irradiation exceeding 9 hours per day and irradiance varies from 5.1 kWh/m$^2$ to 6.3 kWh/m$^2$ [3]. Historically, PVT collectors have been employed to enhance the efficiency of PV panels and harness thermal energy for alternative applications. A study examined these systems in Niger and found that the results were satisfactory [4]. Thus, adequate availability of solar energy and saline water is essential for the successful implementation of solar desalination technology.

Many studies have been done in this field through the last decade following earlier studies of Fath et al. and Erdil et al. It is notified from a work conducted on the thermal efficiency of an MD-based distillation system [1] that the daily quantity of drinkable water generated was equaled to eleven liters per m$^2$ of the absorber surface with an energy of 7.25 kWh per day [1]. A photovoltaic thermal system tested in Cyprus [2] demonstrated that the daily electrical and thermal energy generated respectively were 7 kWh/day and 2.8 kWh/day with an impressive return of investment (ROI) of less than two years [2].

Hughes et al. [5] studied the efficiency of an MD structure-based concentration photovoltaic/thermal system. The result from this experimentation shows that the highest amount of flux produced is 3.41 L/m$^2$. The conductivity of distillated H2O reduces from 35 µs/cm. The transient operation of the membrane was not affected by the variation of the distillate flow rate.

An investigation on DCMD efficiency was conducted by Sulaiman et al. [6] to determine the mass flux and the thermal efficiency. It was reported that there is a proportional relation between the temperature gradient, flux, and thermal efficiency. Better performance of DCMD was obtained while utilizing polymeric membranes at 0.7 mm and high porosity. The mass flux and thermal power were 26% and 50%, respectively. From the economic analysis, the cost of distilled water generated via reverse osmosis was found to be around $0.50 per m$^3$.

Kelley et al. [7] conducted a study on PV-energized RO structures used for providing fresh water in rural, isolated areas. It was observed that thermal control may augment the production of fresh water. Concentrating mirrors are included in the stated structure to increase electrical efficiency and cool the solar panel. The freshwater production increases up to 59%. AGMD-associated solar system was analyzed by Burrieza et al. [8]. The concentration of the saline water and its temperature were 35 g/L and 80 °C. The maximum portable water produced was around 7 L/m$^2$.h, and the higher thermal efficiency and energy consumption were 79% and 810 kWh/m$^3$.

Distillation solar system with an MD studied by Koschikowski et al. [9] reported that the capacity of the system was between 100 and 500 L per day. The maximum evaporator inlet temperature and distillate flow were 85 °C and 15 L/h.

An economic analysis of MD and other desalination techniques was done by Kesieme et al. [10]. The result showed that the RO recovery can be improved using MD. Reverse osmosis is expensive; however, with the price of carbon, the cost of the desalination system augments while the RO remains intact. In addition, membrane distillation was found to be more economical than other techniques, with a cost of $0.66 per $m^3$. Mittelman et al. [11] investigated water desalination systems combined with concentrating photovoltaic-thermal collectors. The yearly amount of heat supplied to the MEE was recorded to be around 3%. The water outflow temperature from the CPVT collector was 90 °C, and the specific energy consumption of MEE is 62 kWh/$m^3$.

CPVT system combined with DCMD for desalinating seawater is investigated by Hrari et al. [12]. The average electrical and thermal efficiencies are 18% and 71%, respectively. The production of portable water is 3 kg/$m^2$ per hour, and the required thermal energy is approximately 9200 kJ/kg water.

Using a PVT system, a study is conducted by Aswathi et al. [13] on a dual-slope desalination unit. They enhanced the efficiency of this model by 50%, achieving better performance at higher glass cover temperatures, primarily at maximum irradiance.

Balachandran et al. [14] have improved the solar still-based PVT structure by using a cooling H2O film system and HNFC insulation. The production of freshwater is 2.253 L/$m^2$ per day when the depth of the HNFC insulation is 0.5 cm and 1.420 L/$m^2$ when the insulation depth equals 1 cm. A stepped PVT solar still possessing a bottom channel is investigated by Xiao et al. [15]. When this channel is around 0.01 m, the temperature of feed water increases by 16.4%. Furthermore, reports indicate a 44% enhancement in the average heat transfer. Also, the amount of distilled water produced per day increased by 51.7%. The average exercise and thermal efficiencies are raised by 3% and 17%, respectively.

Rafiei et al. [16] conducted a study on a hybrid solar desalination system using different types of cavity receivers and a humidifier and dehumidifier system. The maximum freshwater yield was recorded to be 19 kg per hour when the oil inlet temperature is 40 °C and 0.42 kg/s for the highest water flow rate.

Singh et al. [17] evaluated an experimental purification water structure consisting of SS-based dual photovoltaic/thermal collectors. They observed an increase in the annual production of clean water, ranging from 120.29% to 883.55%. The highest production cost for freshwater was around Rs.4.08 per kg.

Gaur et al. [18] investigated the required quantity of absorbers in the HASS-PVT system. The results indicated that 4 collectors are required for every 50 kg of mass water. The daily freshwater production was 7.9 kg, which was higher than the passive one's. The analysis of SS associated with many identical PVT structures is studied by Singh [19]. The annual production of freshwater was obtained when the water depth was around 0.14 m. The cost production of freshwater of N-PVT-FPC-SS was enhanced by 27.5%.

Naroei et al. [20] discussed the efficiency of stepped SS integrated with PVT collectors. The integration of stepped SS with PVT collectors enhances freshwater production by 20%, resulting in a daily production of approximately 5.71 kg/$m^2$. It was found that the PVT collector supplied an extra electrical power of 1.06 kW per day. The efficiency of different designs of solar still for industrial and domestic applications was presented by Katekar et al. [21]. The enhancement in production of water of one and dual basin SS solar still were 112% and 127.65% respectively. The maximum improvement in the production of freshwater was around 67.6%.

Xinxin et al. [22] explored another method of producing drinkable water using the LCPV/T SS system. The highest exergy efficiency is 15.50% and 14.02% of the average exergy. The maximum freshwater yield was reported to be 917.3 g per day, with a slope of 45 °C. According to the economic analysis, the price of freshwater is around ¥0.0095 per liter, with an IRR value of 14.59%.

An analytical expression of dual SS coupled with different PV/T-FPC operating with and without helical heat exchanger was created by Sahota et al. [23]. The system using nanofluid yields freshwater in the range of 4.54 kg to 5.25 kg.

The adsorption desalination system integrated with a PVT module was explored by Mohamed Ghazy et al. [24]. In the afternoon, the maximum electrical and thermal efficiencies were 11.5% and 77.5%, respectively. Coefficient of performance (COP), specific cooling power, and desalinated water were also investigated. Thus, the maximum daily freshwater produced was 6.3 $m^3$/ton.

Sharma et al. [25] conducted an analytical study on the dissimilarity of the mass flow rate on SS associated with different PV/T structures. The highest exergy on enviro-economic parameters was observed at N= 10 m and N= 0.14 m. The highest energy of the structure is observed at N= 6 kg/s and N= 0.10 kg/s.

Another study was done by Abozoor et al. [26] on active SS associated with evacuated flat plate structure. The useful energy registered during the day for one and two glass cover glass EFPC was 45.85% and 46.64%, whereas the exergy efficiency of these systems is 7.95% and 8.21%, respectively. The single-cover glass EFPC produced 17.45 kg of distilled water per day, while the double-cover glass EFPC produced 17.97 kg. Rafeek et al. [27] analyzed the efficiency of an inclined SS-embedded solar panel absorber at different mass flow rates. Thus, at m= 8 kg/h, the maximum quantity of freshwater collected equaled 8.1 kg/h. However, the maximum electrical, thermal, and exergy efficiencies were recorded as follows: 20.03%, 22.21%, and 23.36% for m= 4.7 kg/h.

In an attempt to improve the desalination system, a reverse osmosis (RO) using saline water and a PV system was investigated in Egypt [28]. The four methods employed revealed a 14.3% increase in the photovoltaic panel's electrical efficiency using 203 L/$m^2$ of freshwater. In certain Middle Eastern and North African countries, researchers conducted another theoretical study using the PVT-RO desalination system [29]. Thus, the PVT system's electrical efficiency increased by 8%, while its specific energy consumption registered at 0.135 kWh/$m^3$.

Hemmatian et al. [30] conducted an experimental study using phase change material (PCM) and solar collectors to improve the performance of solar still systems. They reported collecting 2.248 L/$m^2$ of distilled water per day, with an estimated production cost of 0.0458 dollars per liter.

Nanofluids were also utilized to improve the efficiency of desalination systems. Thus, PVT-CPC using SWCNTs and MWCNTs water nanofluids were examined [31]. This system improved its efficiency by up to 30% compared to the baseline, establishing SWCNTs as another reliable solution.

These works clearly show that only a limited number of investigations have taken place in Africa, specifically in North Africa. Thus, this study aims to analyze the performance of a solar still system combined with a PVT module in Niger's climatic conditions. This study marks the inaugural investigation in Niger, specifically in the West African region.

## 2. Mathematical Modeling

The solar desalination system used in this study is a single slope solar still based-PVT collector as depicted in the below Fig. 1. The system is composed of a PVT collector, a pump, and a solar still. When the solar irradiance increases, the temperature of the PV module increases, and as a result, its electrical efficiency decreases. Thus, the cooling of the photovoltaic module and enhancement of its efficiency are carried out by saline water, which is passed through the thermal collector fixed at the backside of the solar panel. The feed water is heated, then circulated via a pump in the solar still. The solar still operates using the incalescence effect: the solar radiation causes water to be vaporized inside a glass-lined enclosed space at a temperature greater than the room temperature. The preheated feed water temperature increases due to sun radiation, and it starts evaporating at a certain temperature. The water vapor condenses to produce distilled droplets of water as cooling at the surface of the glass. These droplets slide down along the glass's surface and are gathered in a container, ready to be used.

This system is a self-powered system where some of the generated electrical power of the PV module is utilized to power the pump, and the remaining part can either be sent to the grid or power some devices such as a radio, DC lamp, etc. The thermal and electrical efficiencies of the PVT collector were investigated here by identifying the temperatures of the glass cover and evaporated water, as well as conducting an energy analysis of the photovoltaic-thermal collector and solar still.

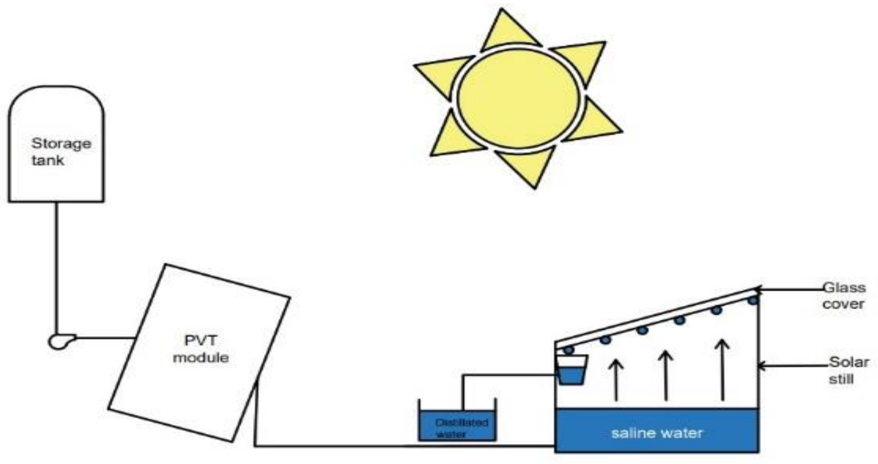


**Figure 1:** Schematic display of SS still integrated PVT module.

### 2.1. Energy Analysis of PVT System

The effective energy $Q_u$ of the collector is given as the difference between the absorbed solar irradiance and the heat loss from the collector [32]:

$$Q_u = A_c F_R [G - U_L (T_i - T_a)] \tag{1}$$

Where Ac, G, $T_a$, $T_i$ and $U_L$ are the collector area, solar radiation, ambient temperature, inlet water temperature and heat loss coefficient, respectively. And $F_R$ is the heat removal factor collector which can be deducted as follows [32]:

$$F_R = \frac{\dot{m}C_p}{A_C U_L}[1 - \exp -(\frac{A_C U_L F\prime}{\dot{m}C_p})] \quad (2)$$

The output electrical power is determined by this formula:

$$P_{el} = V_{oc} I_{sc} FF \quad (3)$$

where $V_{oc}$ *and* $I_{sc}$ are open circuit voltage and short circuit current of the PV panel itself. FF stands for fill factor which is a measure on squareness of the typical IV curve of a PV panel. The electrical efficiency as well as the thermal efficiency of the given system are determined using the equations below [32]:

$$n_{el} = n_r[1 - \beta(T_{cell} - T_r)] - n_{pump} \quad (4)$$

$$n_{ti} = \frac{Q_u}{GA_c} = F_R(\tau\alpha) - F_R U_L \frac{(T_i - T_a)}{G} \quad (5)$$

Where $n_{pump}$, $U_L$, *and* $F'$ are the efficiency of the pump, heat loss coefficient and the collector efficiency factor. The expression of $U_L$, $n_{pump}$ and $F'$ are transferred to the Appendix section to avoid complexity in the text-flow.

### 2.2. Energy Analysis of Solar Still

For the solar still in the current study, the glass cover's temperature, evaporated water, and freshwater production are evaluated. The energy balance equation of glass cover is as follows [33, 34]:

$$\alpha_g G A_g + h_{w-g} * A_w * (T_w - T_g) - h_{c,g-a} A_g (T_g - T_a) - h_{r,g-sky} A_g (T_g - T_{sky}) = m_g * C_g * \frac{dT_g}{dt} \quad (6)$$

Where $h_{w-g}$, $h_{c,g-a}$, $h_{r,g-sky}$ represent the total heat transfer coefficient from the briny water surface to the glass cover, convection heat transfer coefficient of the wind on the outer surface of glass cover, and radiative heat transfer coefficient of the outer surface cover of glass cover to the sky. All the expressions of the above heat transfer coefficients are given in the Appendix to avoid complexity in the text-flow. The energy balance equation for briny water is expressed by:

$$\alpha_w \tau_g G A_w + Q_u - h_{w-g} A_w (T_w - T_g) = m_w C_w \frac{dT_w}{dt} \quad (7)$$

The freshwater production rate is determined as follows [33, 34]:

$$m_{ev} = 3600 h_{ev,w-g} \frac{(T_w - T_g)}{L_w} \quad (8)$$

With $m_{ev}$ as mass rate of freshwater, and evaporative heat transfer coefficient ($h_{ev,w-g}$) from the evaporated briny water sheet and its expression is given in the Appendix. $L_w$ represents the latent heat of water vaporization (J/kg) and is expressed as follows [35]:

$$L_w = 2.4935(10^6 - 947.79T_w + 0.13132T_w^2 - 0.0047974T_w^3) \quad (9)$$

The overall thermal efficiency of PVT-SS is determined by the following equation [33]:

$$n_{th} = \frac{\sum m_{ev} \times L_w}{GA_s \times 3600} \times 100 \quad (10)$$

The simulation of this system is done using MATLAB code and weather data of Niamey city. The required design parameters of the PVT collector and solar still are given in Table 1 and Table 2 below.

**Table 1:** Design parameters of PVT system

| Parameters | Values | Parameters | Values |
|---|---|---|---|
| Ta | 293 K | Pmax | 150 W |
| Ep | 0.95 | Vmp | 17.2 V |
| Ec | 0.88 | Imp | 8.72 A |
| N | 1 | Voc | 21.6 V |
| M | 0.07 kg/s | Isc | 9.92 A |
| Ac | 1.36 $m^2$ | Isc temp. Coeff | (0.065 ±0.015) %/°C |
| P | 4.85 m | Voc temp. Coeff | -(80 ±10) mV/°C |
| $V_{wind}$ | 1 $m^2/s$ | Peak power temp. Coeff | -(0.5 ±0.05) %/°C |
| $(\tau\alpha)$_PV | 0.74 | NOCT | 47±2 °C |
| Lab | 0.002 m | Operating temp. | -40 °C to 85 °C |
| Kab | 390 W/m. k | h_pva | 45 $W/m^2K$ |
| Lpv | 0.04 m | Ledge | 0.025 m |
| Kpv | 90 W/m. k | Kedge | 0.045 W/m. k |
| Li | 0.05 m | W | 0.1 m |
| Ki | 0.045 W/m. k | Do | 0.01 m |

**Table 2:** Design parameters of solar still

| Parameters | Values | Parameters | Values |
|---|---|---|---|
| $K$ | 0.78 W/m°C | $\alpha_w$ | 0.05 |
| $L$g | 0.004 m | $m$w | 3.9 kg |
| $C$w | 4190 kJ/kg°C | $\tau_g$ | 0.95 |
| $\alpha_g$ | 0.05 | Ag | 1.2 $m^2$ |
| Aw | 1 $m^2$ | d | 5 cm |
| Cg | 800 J/ (kg. K) | mg | 4.1 kg |

## 3. Results and Discussion

Data of the climatic order such as the hourly solar irradiance, ambient temperature, and different equations stated above, have been simulated using MATLAB software. These parameters are the primary factors influencing the performance of the PVT collectors. Thus, the hourly solar irradiance along with the ambient temperature for weather conditions of Niamey city on 7th May are used and the results are reported in Fig. 2(a). The irradiance varies from 66 to 970 W/m$^2$, and the temperature is in the range between 33 °C to 45 °C, which alludes to hot weather conditions.

The effects of temperature and irradiation are crucial factors in determining the effectiveness of the photovoltaic panel as presented in Fig. 2(b). There is a progressive rise in electrical power with increasing irradiance, whereas electrical efficiency is oppositely affected. The negative effect of the increasing temperature is more pronounced on the electrical efficiency than the electrical power. It is noticed that at noon, the electrical efficiency of the PVT panel is recorded as 14%, whereas the electrical power at that instant is 184.58 W. This power is sufficient to power the whole system, which makes it a self-power system. Some of this power is supplied to the pump, and the remaining part can be used either to charge a battery or send it to the grid.

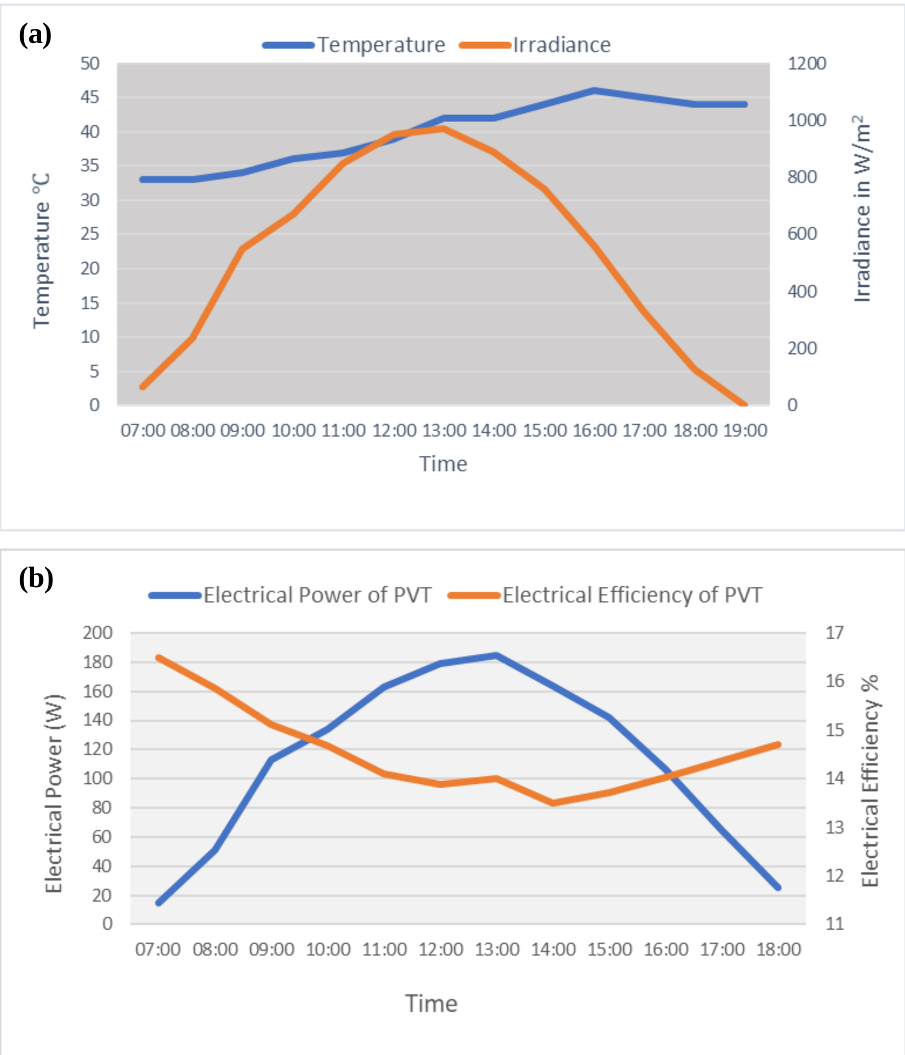


**Figure 1.** Meteorological and PVT system parameters in May of a typical year; **(a)** Ambient temperature and irradiance [3], **(b)** Electrical efficiency and electrical power output of the PVT system

A further investigation is carried out to examine the effect of irradiation on electrical efficiency during the remaining months of the year. The daily fluctuations of these parameters for January and September are illustrated in Fig. 3(a) and Fig. 3(b).

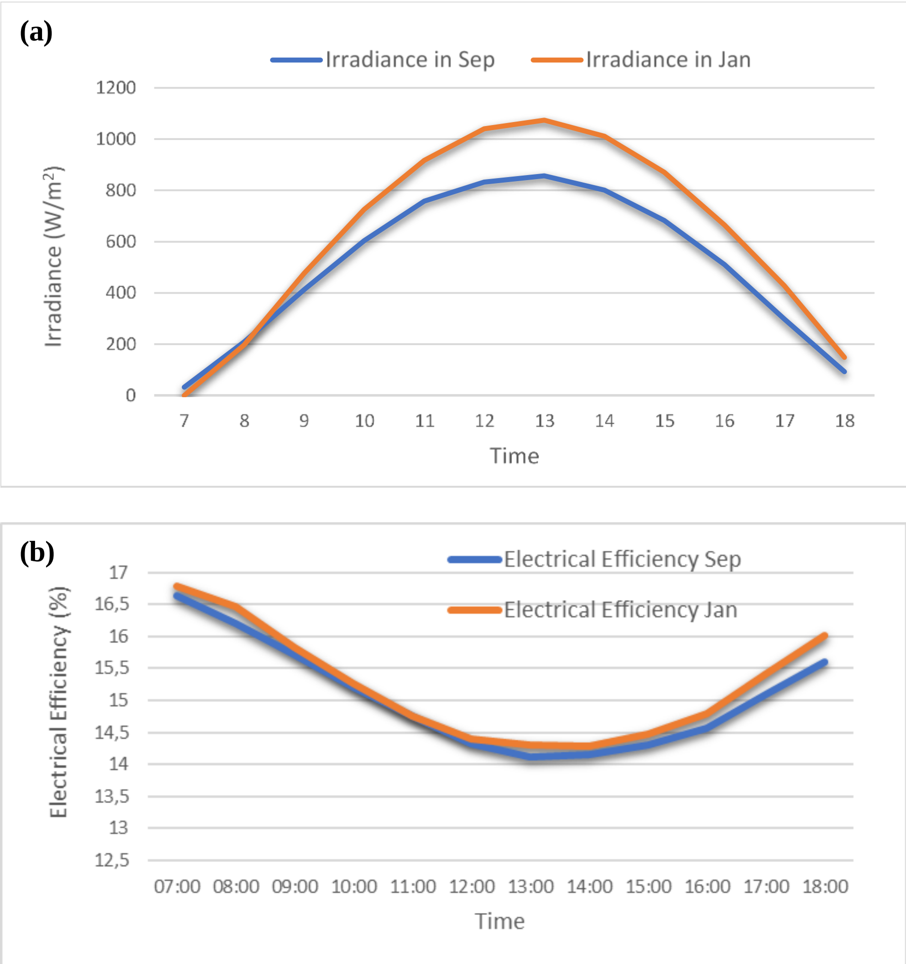


**Figure 3**. **(a)** Variation of solar irradiance in January and September, (**b)** Electrical efficiency of PVT system in January and September.

It is impressive to see that January is in the winter season, whereas September is in the fall season in Niamey/Niger. During the winter and fall, the maximum irradiances are 1073.86 W/m$^2$ and 856.25 W/m$^2$, respectively, as depicted in Fig. 3(a). However, the maximum efficiencies do not differ significantly between these two distinct seasons, 14.12% and 14.3%, respectively, as shown in Fig. 3(b). The nearly vanishing results are due to ambient temperature effects since yielding amplitudes of temperatures in September are lower, acting in favor of electrical efficiency.

We conducted an analysis on the thermal energy side of the PVT collector, and Fig. 4(a) illustrates the hourly fluctuation of thermal power as given in Eq. 1. This demonstrates the desired correlation between solar irradiation and thermal power. The highest recorded thermal power is 879.82 W, which is a significant gain compared to single PV panel technology. The daily variation of thermal efficiency of the solar still associated with PVT in May demonstrated this gain more clearly, as given in Fig. 4(b). Thermal efficiency is quite high, reaching its maximum value of 58.09% at noontime. This implies that the total efficiency of this hybrid PVT-solar still combination, the sum of electrical and thermal efficiencies, is over 72%. Moreover, the amplitude of useful thermal energy triggering the desalination process is largely acceptable compared with available solar still systems, i.e. evacuated solar thermal collectors with flat plate structures [26].

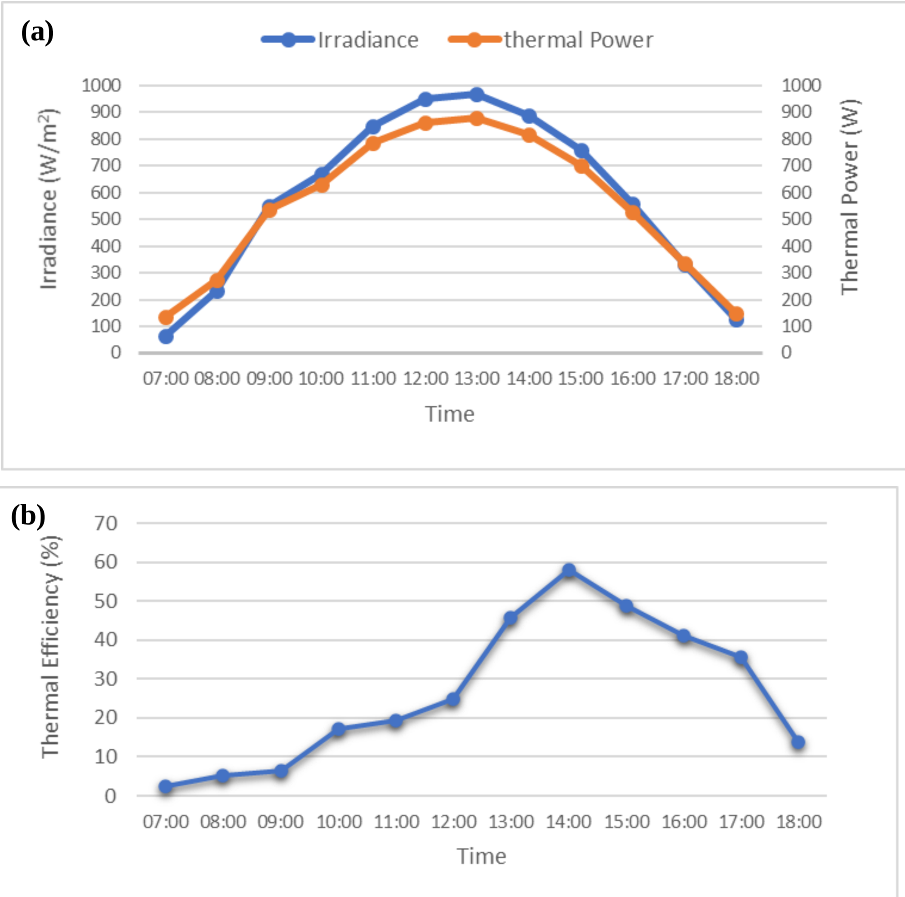


**Figure 4.** Variation of thermal parameters of the PVT in May of a typical year; **(a)** Solar irradiance and thermal power output of the PVT system, *(***b)** Thermal efficiency.

The analysis of heat transfer parameters and water and glass temperatures of solar still itself is primordial to understand the driving mechanism of the freshwater production. Fig. 5(a) illustrates the hourly variations in the temperatures of the solar still's glass cover and the accumulated water in the solar still for the month of May. A water depth of 0.5 cm is considered optimal, as evaporated water output decreases with increasing water depth. The maximum temperature reached by the water in the solar still is 60.5 °C, while the glass cover reaches 51.4 °C. A larger temperature difference here is desired, as it serves as the primary driving mechanism for freshwater production.

This aspect of the system can be verified by evaluating convective and radiative heat transfer coefficients within and on the glass surface of the solar still, as depicted in Fig. 5(b). The results show that the evaporative convection heat transfer coefficient ($h_{ev,w-g}$) is a dominant factor for determining the rate of freshwater production as stated by earlier studies [33, 34]. The maximum value of this heat transfer coefficient is 79.15 W/(m$^2$K) recorded around noon (at 14:00), which is consistent with the time when the maximum temperature difference between $T_w$ (water temperature) and $T_g$ (glass temperature) is obtained (see Fig. 5(a)).

Fig. 6 depicts the variation in the freshwater production rate in May, allowing us to observe whether the rates align with the previously claimed driving mechanism. The highest measurable amount of freshwater is 1.1 kg/m$^2$/h, observed at around noontime (at 14:00). This is clear confirmation of that the evaporative heat transfer coefficient ($h_{ev,w-g}$) and the temperature difference between the water and glass cover largely influence the yield. The production starts at 10:00 AM and lasts nearly 7 hours, just before sunset time. The daily freshwater yield reaches 2.62 kg/m$^2$, in addition to the electrical power produced by the PV panel side of the system.

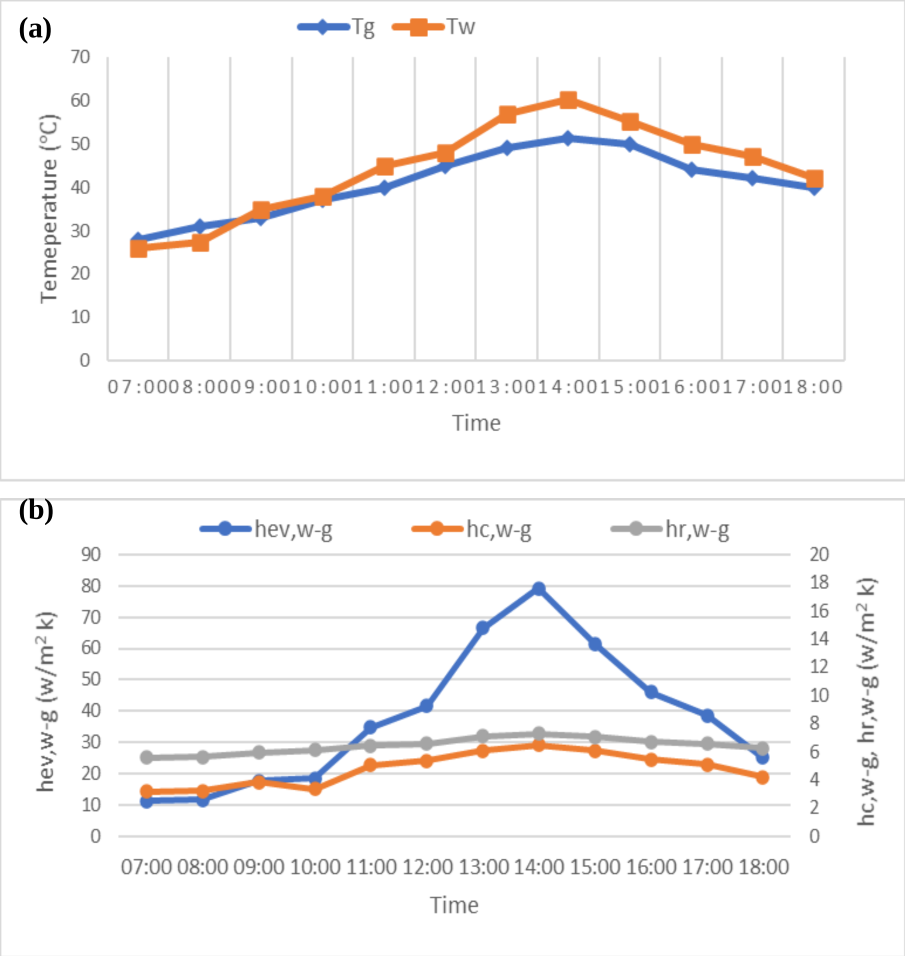


**Figure 5.** Variation of temperature and heat transfer parameters of the SS solar still in May of a typical year; (a) Water and glass cover temperatures, (b) Convective and radiative heat transfer coefficients.

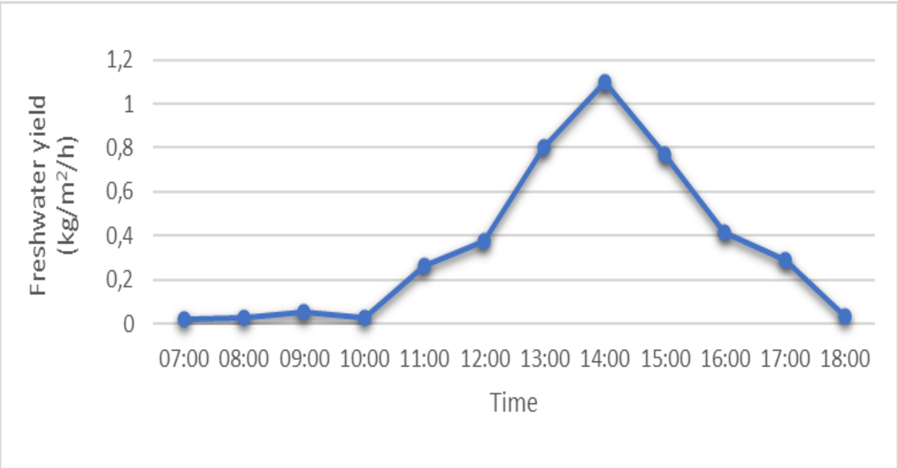


**Figure 6.** Variation of fresh-water production rates of the SS solar still in month of May in a typical year.

Next, we provide the results of the comparable analysis conducted for January and September in Fig. 7. In terms of the dominating effect of evaporative convection heat transfer coefficient $(h_{ev,w-g})$, our data are constant and consistent as the maximum production rates corresponded well with the period when amplitudes of $(h_{ev,w-g})$ reached their highest value. This time slightly changes with the season, earlier in January (at 13:00 compared to 14:00 in September). The maximum freshwater yields in September and January are recorded as 0.48 kg/m$^2$/h and 0.389 kg/m$^2$/h respectively.

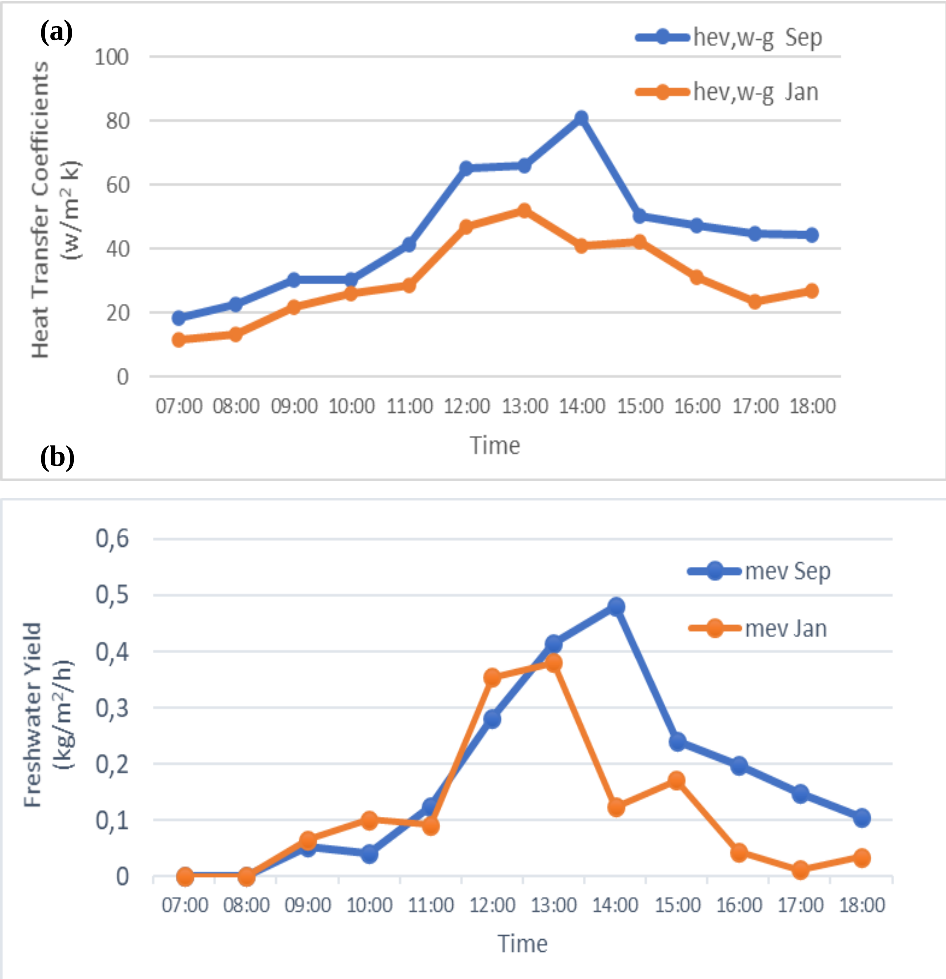


**Figure 7.** Variation of selected yields of the SS solar still in the months of January and September of a typical year; (a) Evaporative convection heat transfer coefficient, (b) Fresh-water production rates.

Table 3 presents a comparative analysis of our present study and other studies that were included in the literature review. The table unequivocally illustrates the sufficiency of our work, considering that the system utilized in this study is a single-slope solar still. The results are substantial and provide possible solutions to the water scarcity problem in Niger. Given the current economic conditions in Niger, the results of this study, which is the first investigation of the single-slope solar still combined with PVT module, are mostly satisfactory.

**Table 3:** Comparative assessment of present research with previous studies

| Authors | System Type | Daily Freshwater Yield |
|---|---|---|
| Gaur et al. [18] | HASS-PVT system | 7.9 kg/m$^2$ |
| Naroei et al. [20] | Stepped SS integrated with PVT collectors. | 5.71 kg/m$^2$ |
| Balachandran et al. [14] | Solar still -based PVT system with HNFC insulation | 2.253 L/m$^2$ |
| Hemmatian et al. [30] | Solar still integrated PCM and solar collectors | 2.248 L/m$^2$ |
| Present Study | Single Slope Solar Still integrated PVT collector | 2.62g/m$^2$ |

## 4. Conclusion

Water shortage is a global issue, and desalination is used to provide potable water for humans and animals. Research is being conducted on solar stills equipped with photovoltaic thermal collectors to enhance freshwater production. Niger, a developing nation with 70% of its superficies being a desert, is exploring the use of integrated solar still systems to provide potable water in regions with limited energy and water resources.

Using an average daily solar irradiation of 9 hours, this work examines the efficiency of a photovoltaic-thermal (PVT) collector integrated solar still system in Niamey, Niger. The analysis encompasses the electrical and thermal efficiency of the PV/T structure, along with a temperature analysis of the water and glass cover system, and a computation of freshwater generation. Thus, the maximum electrical power and thermal power at noontime are determined to be 184.56 W and 879.82 W, respectively.

The photovoltaic/thermal (PV/T) system used here has an overall efficiency of 72%, a sum of 14% electrical efficiency and 58.09% thermal efficiency. The temperature of water within the solar still ranges from 26 °C to 60 °C. The maximum daily freshwater production is 2.62 kg/m$^2$. These findings are found to be well within the boundaries of earlier studies.

The implementation of this system can effectively mitigate the water issue in these isolated regions and improve the availability of electricity to the population. This is particularly important because the geological characteristics of these areas prevent the electrical grid lines from reaching them. Consequently, these isolated regions have difficult and severe living circumstances. An optimal solar still-integrated PVT collector has great potential to enhance the availability of potable water and electricity in African countries. An optimal solar still-integrated PVT system has thus great potential in enhancing the availability of potable water and electricity in African countries.

Potential future scientific investigations may involve the utilization of nanofluids to elevate the temperature of saline water in a double-slope solar still, as well as the integration of appropriate phase change material (PCM) into the container to continue distilled water production at later evening hours.

From the practical application side, this hybrid system can be installed at a larger commercial scale, ranging between $10^2$and $10^3$ kW electrical power levels. Based on our findings, this scale will allow desalination of nearly 1-10 tons/day of water from rivers throughout the country, in addition to providing electricity for 80-800 neighboring homes.

## 5. Appendix: Supplementary equations for the analysis given in the Section 2.

$$P_p = \frac{m_f \Delta P}{\rho_f n_p}$$

$$F' = \frac{1}{\frac{W U_L}{\pi D i h} + \frac{W}{Do + (W - Do)F} + \frac{U_L}{W h_{pva}}}$$

$$F = \frac{\tanh[m(W - Do)/2]}{m(W - Do)/2}$$

$$m = \sqrt{\frac{U_L}{kL}}$$

$$U_L = U_t + U_e + U_b$$

$$T_{Pm} = T_{f,i} + \left(\frac{Q_u/A_c}{U_L F_R}\right)(1 - F_R)$$

$$U_t = \left[\frac{N}{\frac{C}{T_{pm}}\left(\frac{T_{pm} - T_a}{N + f}\right)^e} + \frac{1}{h_w}\right]^{-1} + \frac{k(T_{pm} + T_a)(T_{pm}{}^2 + T_a{}^2)}{(\varepsilon_p + 0.00591 N h_w) + \frac{2N + f - 1 + 0.133\varepsilon_p}{\varepsilon_g} - N}$$

$$h_w = 5,7 + 3,8 * V_{wind}$$

$$C = 520(1 - 0.000051(\theta)^2)$$

$$e = 0.43\left(1 - \frac{100}{T_{pm}}\right)$$

$$f = \left(1 + 0.089 h_w - 0.1166 h_w \varepsilon_p\right).(1 + 0.07866 N)$$

$$U_b = \frac{k_i}{L_i}$$

$$U_e = \frac{k_{edge} . p . t}{L_{edge} . A_c}$$

$$h_{ev,w-g} = 0.01623 h_{c,w-g}\left(\frac{P_w - P_g}{T_w - T_g}\right)$$

$$h_{c,w-g} = 1.22\left(\frac{k_v}{d}\right)(\dot{G}_r Pr_v)^{0.22}$$

$$\dot{G}_r = \frac{\beta_v g d^2 \rho_v^2 \Delta\dot{T}}{\mu_v^2}$$

$$\Delta\dot{T} = \frac{(T_w - T_g) + (P_w - P_g)(T_w + 273)}{(268.9 * 10^3 - P_w)}$$

$$P_w = exp\left[25.317 - \frac{5144}{T_w+273}\right]$$

$$P_g = exp\left[25.317 - \frac{5144}{T_g+273}\right]$$

$$Pr_v = \frac{\mu_v C_v}{k_v}$$

$$C_v = 999.2 + 0.143T_w + 1.0101 * 10^{-4}T_w^2 - 6.7581 * 10^{-8}T_w^3$$

$$T_L = \frac{T_w+T_g}{2}$$

$$\rho_v = \frac{353.44}{T_L+273}$$

$$k_v = 0.0244 + 0.7673 * 10^{-4}T_L$$

$$\beta_v = \frac{1}{T_L+273}$$

$$\mu = 1.718 * 10^{-5} + 4.62 * 10^{-8}T_L$$

## References


[1] Fath, H.E., et al., PV and thermally driven small-scale, stand-alone solar desalination systems with very low maintenance needs. Desalination, 2008. 225(1-3): p. 58-69.

[2] Erdil, E., M. Ilkan, and F. Egelioglu, An experimental study on energy generation with a photovoltaic (PV)–solar thermal hybrid system. Energy, 2008. 33(8): p. 1241-1245.

[3] Dankassoua, M. and S. Yahaya, Evaluation of Solar Potential at Niamey: Study Data of Insolation from 2015 and 2016. Smart Grid and Renewable Energy, 2017. 8(12): p. 394-411.

[4] Garba, M.A., Performance Analysis of Photovoltaic-thermal (PV/T) Solar Systems. 2020.

[5] Hughes, A., T. O'Donovan, and T. Mallick, Experimental evaluation of a membrane distillation system for integration with concentrated photovoltaic/thermal (CPV/T) energy. 2014.

[6] Al-Obaidani, S., et al., Potential of membrane distillation in seawater desalination: thermal efficiency, sensitivity study and cost estimation. Journal of Membrane Science, 2008. 323(1): p. 85-98.

[7] Kelley, L.C. and S. Dubowsky, Thermal control to maximize photovoltaic powered reverse osmosis desalination systems productivity. Desalination, 2013. 314: p. 10-19.

[8] Guillén-Burrieza, E., et al., Experimental analysis of an air gap membrane distillation solar desalination pilot system. Journal of Membrane Science, 2011. 379(1-2): p. 386-396.

[9] Koschikowski, J., et al., Experimental investigations on solar driven stand-alone membrane distillation systems for remote areas. Desalination, 2009. 248(1-3): p. 125-131.

[10] Kesieme, U.K., et al., Economic analysis of desalination technologies in the context of carbon pricing, and opportunities for membrane distillation. Desalination, 2013. 323: p. 66-74.

[11] Mittelman, G., et al., Water desalination with concentrating photovoltaic/thermal (CPVT) systems. Solar Energy, 2009. 83(8): p. 1322-1334.

[12] Al-Hrari, M., et al., Concentrated photovoltaic and thermal system application for fresh water production. Applied Thermal Engineering, 2020. 171: p. 115054.

[13] Aswathi, G. and V. Rajesh. Design and Experimentation of Double Slope Desalination Unit Coupled with Photovoltaic Thermal Collector. in IOP Conference Series: Materials Science and Engineering. 2019. IOP Publishing.

[14] Balachandran, G.B., et al., Enhancement of PV/T-integrated single slope solar desalination still productivity using water film cooling and hybrid composite insulation. Environmental Science and Pollution Research, 2019: p. 1-12.

[15] Xiao, L., et al., Performance study on a photovoltaic thermal (PV/T) stepped solar still with a bottom channel. Desalination, 2019. 471: p. 114129.

[16] Rafiei, A., et al., Thermal analysis of a hybrid solar desalination system using various shapes of cavity receiver: Cubical, cylindrical, and hemispherical. Energy Conversion and Management, 2019. **198**: p. 111861.

[17] Singh, D., et al., Experimental studies of active solar still integrated with two hybrid PVT collectors. Solar Energy, 2016. 130: p. 207-223.

[18] Gaur, M., et al., Integrated PVT Hybrid Active Solar Still (HASS) with an Optimized Number of Collectors, in Solar Desalination Technology. 2019, Springer. p. 219-236.

[19] Singh, D., Improving the performance of single slope solar still by including N identical PVT collectors. Applied Thermal Engineering, 2018. 131: p. 167-179.

[20] Naroei, M., F. Sarhaddi, and F. Sobhnamayan, Efficiency of a photovoltaic thermal stepped solar still: experimental and numerical analysis. Desalination, 2018. 441: p. 87-95.

[21] Katekar, V.P. and S.S. Deshmukh, A review on research trends in solar still designs for domestic and industrial applications. Journal of Cleaner Production, 2020: p. 120544.

[22] Xinxin, G., et al., Experimental and theoretical investigation on a hybrid LCPV/T solar still system. Desalination, 2019. 468: p. 114063.

[23] Sahota, L. and G. Tiwari, Analytical characteristic equation of nanofluid loaded active double slope solar still coupled with helically coiled heat exchanger. Energy Conversion and Management, 2017. **135**: p. 308-326.

[24] Ghazy, M., et al., Experimental investigation of hybrid photovoltaic solar thermal collector (PV/T)-adsorption desalination system in hot weather conditions. 2022: p. 124370.

[25] Sharma, G.K., et al., An investigation on dissimilarity of mass flow rate and N on exergo-enviro-economic parameters for solar still of single slope type integrated with N similar PVT flat plate collectors having series connection. 2022: p. 1-18.

[26] Abozoor, M.K., et al., Energy and exergy analyses of active solar still integrated with evacuated flat plate collector for New Delhi. 2022. 19: p. 100833.

[27] Rafeek, M.T.M., et al., Experimental investigation of an active inclined solar panel absorber solar still—energy and exergy analysis. 2022. 29(10): p. 14005-14018.

[28] Abdelrahman, M., et al., Improving the performance of a PV-RO brackish water desalination plant in Egypt using solar thermal feed preheating technology. Journal of Energy Storage, 2024. 98: p. 113115.

[29] Bacha, H.B., et al., Performance analysis and techno-economic assessment of a developed cooling/preheating small PVT-RO desalination plant. Frontiers in Energy Research, 2023. 11: p. 1287743.

[30] Hemmatian, A., et al., Improving solar still performance with heat pipe/pulsating heat pipe evacuated tube solar collectors and PCM: An experimental and environmental analysis. Solar Energy, 2024. 269: p. 112371.

[31] Arora, S., et al., Energy matrices, enviro-economic and characteristic equation-based performance analyses of photovoltaic thermal compound parabolic concentrator (PVT-CPC) coupled solar still equipped with heat exchanger using SWCNTs and MWCNTs–water nanofluids. International Journal of Ambient Energy, 2024. 45(1): p. 2308039.

[32] Iordanou, G., Flat-plate solar collectors for water heating with improved heat transfer for application in climatic conditions of the mediterranean region. 2009, Durham University.

[33] Dashtban, M. and F.F. Tabrizi, Thermal analysis of a weir-type cascade solar still integrated with PCM storage. Desalination, 2011. 279(1-3): p. 415-422.

[34] Zoori, H.A., et al., Comparison between energy and exergy efficiencies in a weir type cascade solar still. Desalination, 2013. 325: p. 113-121.

[35] Kumar, S. and A. Tiwari, An experimental study of hybrid photovoltaic thermal (PV/T)-active solar still. International Journal of Energy Research, 2008. 32(9): p. 847-858.